CHEMISTRY OF MATERIALS

ARTICLE

pubs.acs.org/cm

Formation of TiO_2 Nanostructures by Enzyme-Mediated Self-Assembly for the Destruction of Macrophages

Koichiro Hayashi,*,† Michihiro Nakamura,† Wataru Sakamoto,‡ Toshinobu Yogo,‡ Toshinari Kori,§ and Kazunori Ishimura†

†Department of Anatomy and Cell Biology, Institute of Health Biosciences, The University of Tokushima Graduate School, 3-18-15 Kuramoto-cho, Tokushima 770-8503, Japan

‡Division of Nanomaterials Science, EcoTopia Science Institute, Nagoya University, Furo-cho, Chikusa-ku, Nagoya 464-8603, Japan

§Tokushima Prefectural Industrial Technology Center, 11-2 Nishibari, Saigacho, Tokushima 770-8021, Japan

Supporting Information

ABSTRACT: Conifer foliage-like rutile TiO_2 nanoparticles (CFR NPs), spherical anatase TiO2 NPs (SA NPs), and a mixture of CFR and SA NPs were synthesized in aqueous solution at low temperature. Furthermore, sea urchin-like nanostructures combining SA and CFR NPs, which were designated as anatase/rutile nanostructures (A/R NSs), were produced through the self-assembly of jack bean urease (JBU). The specific surface area of the A/R NSs was considerably larger than those of the CFR NPs, SA NPs, and commercial TiO_2 (P25). In addition, the amount of reactive oxygen species (ROS) yielded from the A/R NSs was significantly higher than that yielded from CFR NPs, SA NPs, and P25 because of the large surface area of the A/R NSs and a synergistic effect caused by the integration of anatase and rutile phases. The A/R NSs showed no cytotoxicity at concentrations <100 μg/mL, although CFR NPs, SA NPs, and P25 were cytotoxic, probably because of their size and shape. Using the high surface area and the superior photocatalytic activity of the A/R NSs, macrophages were effectively destroyed by UV irradiation for the purpose of treating atherosclerosis. Macrophages were killed more effectively by the A/R NSs than P25. Furthermore, different mechanisms of cell destruction resulting from UV irradiation, A/R NSs, and a combination of both were investigated. The death of cells treated with A/R NSs and exposed to UV irradiation was induced primarily by apoptosis rather than necrosis; cells that were not treated with the NSs died mainly from necrosis.

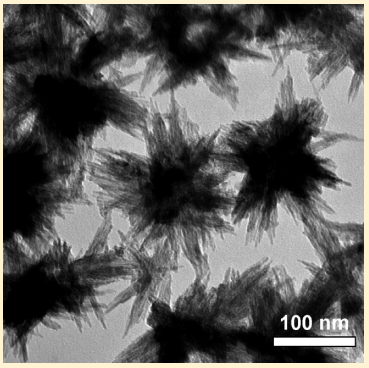

KEYWORDS: titanium dioxide, photodynamic therapy, urease, rutile, anatase

INTRODUCTION

Atherosclerosis is known to cause cerebral infarction, myocardial infarction, and angina, all of which are potentially life-threatening diseases. Therefore, the development of an efficient and effective treatment for atherosclerosis is vital. Atherosclerosis is caused by macrophages that ingest oxidized low-density lipoprotein cholesterol, foam up, and are then deposited on the vascular endothelium.[1,2] Destroying these macrophages could therefore lead to a treatment for atherosclerosis.

Reactive oxygen species (ROS) are able to kill cells by oxidation, and photodynamic therapy (PDT) is a localized treatment that employs ROS.[3] Photosensitizers or light-activated therapeutic moieties such as Photofrin are systematically administered, and then the diseased areas are irradiated with a laser. This results in a high yield of ROS in the diseased area and subsequently results in the destruction of cells. However, because conventional photosensitizers consist of small organic molecules, their diffusion throughout the body has been problematic. The nanoparticulation of photosensitizers is one approach to achieve an accumulation of photosensitizers localized in the diseased area.[4] In addition, conventional photosensitizers yield ROS by irradiation with red light, which does not allow efficient generation of ROS, because it penetrates only a few millimeters into the body, although, of course, the penetration of red light is better than that of UV light. For porphyrins, light with a wavelength of 410 nm is expected to give better results than that with a wavelength of 630 nm.[5] Furthermore, because recent technology allows an affected area to be directly exposed to UV light using a fiber with little scarring, UV light-responsive photosensitizers are now useful for yielding ROS efficiently.

Titanium dioxide (TiO_2) is a promising photosensitizer for PDT because it is able to achieve high yields of ROS owing to its high photocatalytic activity.[6−8] The photocatalytic activity of TiO_2 increases with increasing surface area;, therefore, three-dimensional (3D) nanostructures (NSs) with flower- or sea urchin-like morphology show better activity than spherical particles because of their significantly larger surface area.[9] The photocatalytic activity of TiO_2 also depends on the crystal structure(s) present. It is well-known that crystalline TiO_2 exists in three polymorphs: anatase, rutile, and brookite. In most cases,

Received: March 22, 2011
Revised: May 30, 2011
Published: June 22, 2011

rutile TiO_2 has been shown to exhibit lower photocatalytic activity than anatase TiO_2. Recently, synergistic effects between anatase and rutile nanoparticles (NPs) leading to spatial charge separation and hindered recombination have been proposed to explain the enhanced photocatalytic efficiency of mixed anatase and rutile phases.[10,11] Thus, 3D NSs composed of a mixture of anatase and rutile TiO_2 are promising materials to act as photosensitizers for PDT.

One effective method employed to prepare 3D NSs is self-assembly using biomolecules.[12−15] Jack bean urease (JBU) can be used to control self-assembly because it is a thermostable enzyme that denatures slowly at 60 °C. The activity of JBU at 60 °C is 90% after 4 h, 70% after 12 h, and 50% after 24 h.[16] Such slow denaturation means that aggregation of JBU also progresses slowly, and the degree of aggregation can be easily controlled using the reaction time. Thus, the organization of building blocks into 3D NSs in the presence of JBU can be controlled simply by regulating the reaction time.

In this article, we describe the synthesis methods of spherical anatase TiO_2 NPs (SA NPs), conifer foliage-like rutile TiO_2 NPs (CFR NPs), and a mixture of SA and CFR NPs in aqueous solution at low temperature. We also describe an approach to produce 3D sea urchin-like NSs combining SA and CFR NPs, which were designated as anatase/rutile nanostructures (A/R NSs), via the self-assembly of JBU. Taking advantage of the high surface area and superior photocatalytic activity of the A/R NSs, macrophages were effectively destroyed by the A/R NSs upon irradiation with light for the purpose of treating atherosclerosis. Furthermore, the mechanisms of cell destruction caused by light irradiation, A/R NSs, and a combination of both were investigated.

EXPERIMENTAL METHODS

Synthesis of SA NPs, CFR NPs, and a Mixture of SA and CFR NPs. $TiCl_4$ (60−200 mM, Kishida Chemical Co., Japan) and urea (0−2 M) were dissolved in water, and the solution was then maintained at 40−100 °C for 24 h. The products were collected by centrifugation (20,000*g*) and washed 5 times with water. Synthetic conditions are summarized in Table S1 (Supporting Information).

Formation of A/R NSs. $TiCl_4$ (200 mM), uera (200 mM), and JBU (5.2×10^{-3} mM, Wako Pure Chemical Industries, Japan) were dissolved in Ultrapure water, and the solution was then maintained at 60 °C for 24 h. The products were collected by centrifugation (20,000*g*) and washed 5 times with water.

Structural Analysis. The crystalline phases of the A/R NSs were analyzed by XRD using Cu Kα radiation with a monochromator (Rigaku, RINT-2500 and RINT-Ultima III, Japan). Morphological changes in the products were observed by transmission electron microscopy (TEM, Hitachi, H-760, Japan). The specific surface area of the A/R NSs was measured by the Brunauer−Emmett−Teller (BET) method.

Measurement of the Amount of ROS. The amount of ROS generated by the exposure of an aqueous solution containing 100 μg/mL of A/R NSs, SA NPs, CFR NPs, or P25 (Evonik Industries, Germany) to UV light (365 nm, 1 J/cm^2) for 30 min was measured using a fluorescence spectrophotometer (Hitachi, F-2500, Japan) equipped with a ROS detection kit (Enzo Life Sciences, NY, USA). The detection reagent fluoresced (E_x/E_m = 490/525 nm) in the presence of ROS.

Cytotoxicity Assay without UV Irradiation. Macrophages from C57 BL/6J mice were cultured in an RPMI 1640 medium that was supplemented with 10% fetal bovine serum. A humidified incubator was used with an atmosphere containing 5% CO_2 in air at 37 °C for 24 h. The macrophages were plated in 96-well plates at a concentration of 2×10^5 cells per well and treated with A/R NSs or P25 diluted in RPMI 1640 at 37 °C. Eight wells were used with each condition. After 24 h, the surviving fraction of macrophages was determined by the WST-1 assay.

Table 1. Conditions Used to Treat Cells with A/R NSs and UV Irradiation

condition	treatment with A/R NSs	UV light irradiation	irradiation time (min)
a	−	−	−
b	+	−	−
c	−	+	30
d	+	+	30
e	−	+	90
f	+	+	90

Cytotoxicity Assay with UV Irradiation. The plates were exposed to UV light (365 nm, 1 J/cm^2) after the macrophages were treated with A/R NSs or P25 (100 μg/mL) for 24 h, using an approach similar to that described above. After UV irradiation, the surviving fraction of macrophages was determined by the WST-1 assay.

Cellular Uptake. Fluorescent dye (rhodamine B (RB)) and the A/R NSs were dissolved in water to adsorb RB onto their surface. RB-labeled A/R NSs were washed and centrifuged until no RB was detached from the A/R NSs. To confirm the lack of disassociation of RB in the incubation conditions, we dispersed the RB-labeled A/R NSs in culture solution, centrifuged the solution, and measured the fluorescent intensity of the supernatant solution (E_x = 535 nm). As a result, no fluorescence was detected in the supernatant solution (Figure S1 in Supporting Information). Thus, no RB was detached from the NSs during incubation. The macrophages were treated with the RB-modified A/R NSs for 24 h in an approach similar to that described above. After 24 h, the interaction between the NSs and macrophages was observed using a fluorescence and light microscopy system. This consisted of an inverted fluorescence microscope (TE 2000, Nikon, Kanagawa, Japan) equipped with a 100 W mercury lamp as a light source and a CCD camera (Rolera-XR Mono Fast 1394 Cooled, Qimaging, Burnaby, BC, Canada).

Identification of Apoptosis and Necrosis. Macrophages were incubated with A/R NSs for 24 h and exposed to UV irradiation (365 nm, 1 J/cm^2) under one of the following six conditions (Table 1): (a) not treated with A/R NSs and not exposed to UV irradiation; (b) treated with A/R NSs; (c) exposed to UV irradiation for 30 min; (d) treated with A/R NSs and exposed to UV irradiation for 30 min; (e) exposed to UV irradiation for 90 min; and (f) treated with A/R NSs and exposed to UV irradiation for 90 min. The macrophages were then dyed with annexin V-FITC (BioVision, CA, USA) and 7-AAD-Red (Enzo Life Sciences International, NY, USA), which can detect apoptosis and necrosis, respectively. The macrophages were fixed with 4% formaldehyde and then labeled with DAPI, which is able to dye the DNA in the nucleus of each cell regardless of its status.

RESULTS AND DISCUSSION

Synthesis of SA NPs, CFR NPs, a Mixture of SA and CFR NPs, and A/R NS. SA NPs, CFR NPs, and the mixture of SA and CFR NPs were synthesized by dissolving $TiCl_4$ (60−200 mM) and urea (0−2 M) in water and then heating the solution at 40−100 °C for 24 h. The products were collected by centrifugation and washed 5 times with water. The synthetic conditions used to prepare SA NPs, CFR NPs, and the mixture of SA and CFR NPs are summarized in Table S1 (Supporting Information).

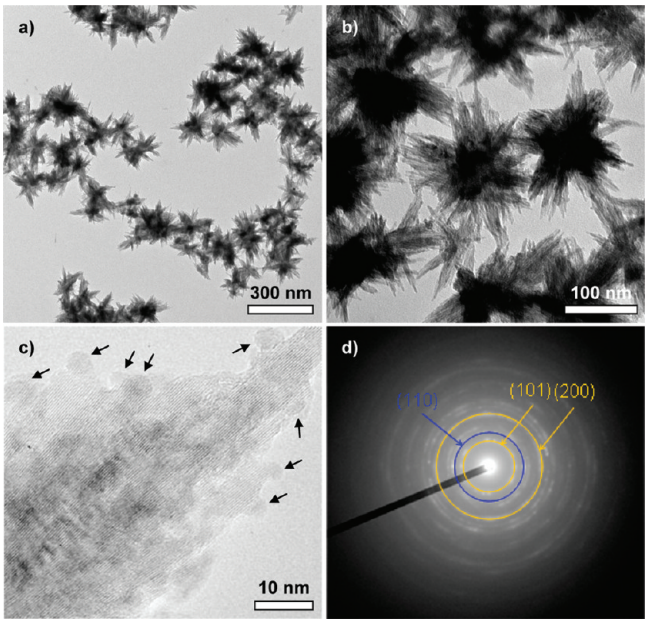

Figure 1. TEM images of (a) A/R NSs, (b, c) magnification of panel a, and (d) SAED pattern of the image in panel c; the blue ring denotes rutile and the yellow rings denote anatase phases.

TEM images revealed that the SA NPs were spherical, with a diameter of 25 nm (Figure S2a, Supporting Information). However, the CFR NPs appeared branched like conifer foliage or a hand-held fan (Figure S2b, Supporting Information). The TEM image of the mixture of SA and CFR NPs shows two kinds of particles with different forms: small spherical particles and conifer foliage-like particles (Figure S2c, Supporting Information). Figure S2d and e (Supporting Information) show a magnified image and the selected area electron diffraction (SAED) pattern of region A, respectively. Spherical particles with a diameter of ~3.5 nm were observed in Figure S2d (Supporting Information), and the SAED pattern of these particles corresponded with that of anatase (Figure S2e, Supporting Information). A magnified image (Figure S2f, Supporting Information) and SAED pattern (Figure S2g) of the conifer foliage-like particles in region B revealed that the crystal structure of these NPs was rutile.

The produce of 3D A/R NSs was straightforward. A water solution of the $TiCl_4$ (200 mM), urea (200 mM), and JBU (5.2×10^{-3} mM) was simply maintained at 60 °C for 24 h. The products were then collected by centrifugation and washed 5 times with water.

TEM images revealed that the long axis of the CFR NPs was oriented toward the center of the sphere, resulting in the formation of sea urchin-like NSs (Figure 1a and b). The mean size of the NSs was 162 ± 15 nm, and the relative standard deviation was 9.4%; thus, the NSs were monodisperse. In addition, spherical particles with a diameter of ~3.5 nm adhered the NSs, as indicated by arrows in Figure 1c. The size of spherical particles coincided with that of the SA NPs observed in Figure S2d (Supporting Information). An SAED pattern of the NSs also established that they consisted of a mixture of SA and CFR NPs because it coincided with the overlapped patterns of anatase (yellow) and rutile (blue) (Figure 1d). Thus, the use of JBU formed the NSs that combined the sea urchin-like rutile framework and spherical anatase nanoparticles, although these were in an unbound state without JBU. Chen et al. reported that urease adheres to particles and causes the particles to self-assemble into spherical superstructures.[17] In general, when an enzyme denatures, its steric structure is lost, and aggregation tends to occur. JBU gradually denatures and aggregates slowly when maintained at 60 °C. Furthermore, it stabilizes the organization of the building blocks into spheres, rather than disordered aggregates at low energies. In this study, as in the work of Chen et al., the self-assembly of CFR and SA NPs into spheres is mediated by JBU, resulting in the formation of sea urchin-like A/R NSs.

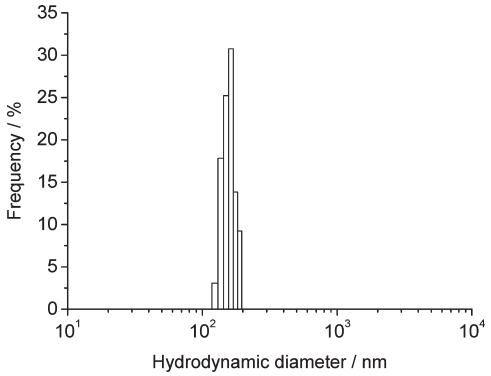

Figure 2. DLS of A/R NSs.

X-ray diffraction (XRD) patterns of SA NPs, CFR NPs, and A/R NSs were consistent with those of anatase, rutile, and anatase/rutile mixed phase, respectively (Figures S3a, b, and c, Supporting Information). The concentrations of precursor and urea and the reaction temperature influenced the crystal structure of the resulting NPs. The anatase/rutile ratio in the NSs estimated from the intensity ratio using a calibration curve was 4/3. It has been reported that this ratio of the two phases provides the maximum photocatalytic activity.[10] In addition, the size of the anatase crystallites in the NSs estimated using the Scherrer equation was 3.3 nm. The crystallite size was coincident with the particle size of anatase in the NSs estimated from TEM observation. The XRD results were consistent with TEM and SAED results and confirmed that the NSs consisted of both SA and CFR NPs.

The hydrodynamic diameter of the A/R NSs measured by dynamic light scattering (DLS) was 151.7 ± 15.1 nm, and the relative standard deviation was 10.0% (Figure 2), which is consistent with the results from TEM (Figure 1).

The specific surface areas of the SA NPs, CFR NPs, and A/R NSs were 100, 130, and 220 m^2/g, respectively. Thus, the self-assembly of a mixture of SA and CFR NPs into A/R NSs led to an increase of the surface area. Furthermore, the specific surface area of the A/R NSs was 4.4 times larger than that of commercial TiO_2 NPs (P25, Evonik Industries) with a diameter of 21 nm and a specific surface area of 50 m^2/g.[18] Like the A/R NSs, P25 also consists of a mixture of anatase and rutile phases.

Generation of ROS by Exposing SA NPs, CFR NPs, A/R NSs, and P25 to UV Irradiation. The amount of ROS generated when SA NPs, CFR NPs, A/R NSs, and P25 were irradiated with UV light was measured using a fluorescent spectrophotometer and a ROS detection kit, where a detectable reagent fluoresced in the presence of ROS (E_x/E_m: 490/525 nm) (Figure 3). The fluorescent intensity of P25 was higher than those of the SA and CFR NPs because of a synergistic effect between the mixture of anatase and rutile phases,[10,11] even though the surface area of P25 was smaller than those of the SA and CFR NPs.

dx.doi.org/10.1021/cm200826c |*Chem. Mater.* 2011, 23, 3341–3347

Furthermore, the fluorescent intensity of the A/R NSs was significantly higher than that of P25 for the following reasons: (1) the A/R NSs had larger specific surface area than P25, and (2) the A/R NSs were more subjected to the electron transfer from rutile particles to anatase particles than P25 because anatase particles and rutile particles in the NSs adhered to each other, although anatase particles and rutile particles in P25 were discretely present.[10] These results demonstrate that both a large surface area and the integration of anatase and rutile phases were important for the efficient generation of ROS.

Cytotoxicity of SA NPs, CFR NPs, A/R NSs, and P25 without UV Irradiation. The cytotoxicity of SA NPs, CFR NPs, A/R NSs, and P25 without the presence of UV irradiation was estimated using a WST-1 assay, which is based on the cleavage of a tetrazolium salt to formazan by cellular mitochondrial dehydrogenases. Figure 4 shows the cell viability of the macrophages against different concentrations of the SA NPs, CFR NPs, A/R NSs, and P25. The cells treated with SA NPs and P25 at concentrations less than 100 μg/mL had a lower survival rate than those treated with A/R NSs and CFR NPs. This indicates that ultrafine particles such as SA NPs and P25 with a diameter of ~25 nm possess higher cytotoxicity than particles with diameters of over 100 nm such as CFR NPs and A/R NSs, and furthermore, that the shape of particles had little influence on cytotoxicity at concentrations of less than 100 μg/mL. Wang et al. also demonstrated that ultrafine TiO_2 NPs induced significant cytotoxicity.[19] However, at concentrations greater than 500 μg/mL, all samples exhibited cytotoxicity. In particular, the viability of cells treated with CFR NPs was significantly decreased. This may have been caused by the 1D shape of the CFR NPs. A/R NSs exhibited low toxicity compared with SA NPs, CFR NPs, and P25 at concentrations of 50−1000 μg/mL and showed almost zero cytotoxicity at concentrations less than 100 μg/mL. The cytotoxicity of the A/R NSs gradually increased as their concentration was increased, but even at a concentration of 1000 μg/mL, over 80% of the cells remained viable. These findings suggest that the self-assembly of 1D particles into 3D NSs or spheres decreases cytotoxicity, even though 1D particles possess cytotoxicity.

Cytotoxicity of UV Irradiation, A/R NSs under UV Irradiation, and P25 under UV Irradiation. The cytotoxicity of A/R NSs and P25, which generated ROS most effectively of the samples investigated, were measured under UV irradiation (365 nm, 1 J/cm^2) by the WST-1 assay (Figure 5). Although exposing the macrophages to UV light resulted in their death, A/R NSs or P25 increased the efficiency of cell death. In particular, macrophages were killed more effectively in the presence of A/R NSs than P25. This is because the A/R NSs have superior photocatalytic activity to P25 and therefore yield more ROS under UV light (Figure 5). Applying UV light to the macrophages for

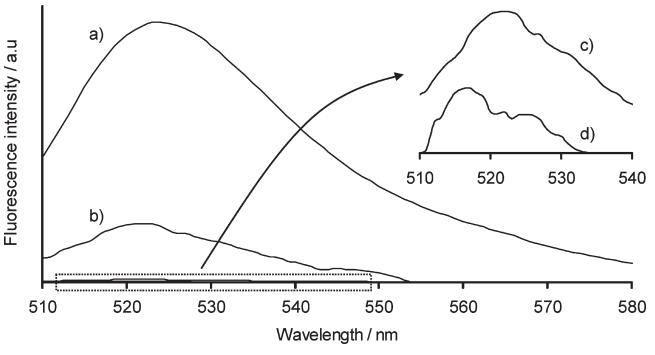

Figure 3. Amount of ROS generated by irradiation of (a) A/R NSs, (b) P25, (c) SA NPs, and (d) CFR NPs with UV light.

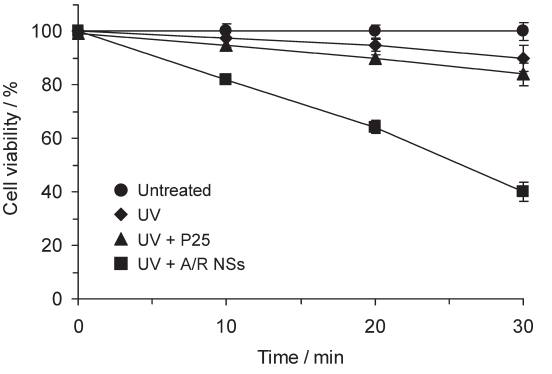

Figure 5. Viability of the cell under the following conditions: no treatment with TiO_2 and no UV irradiation (●); UV irradiation (♦); treatment with P25 and UV irradiation (▲); and treatment with A/R NSs and UV irradiation (■).

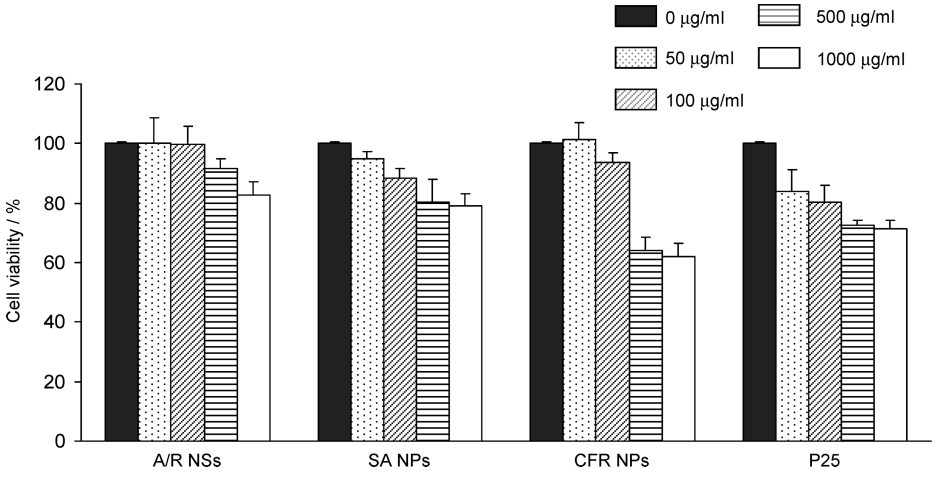

Figure 4. Cytotoxicity of A/R NSs, SA NPs, CFR NPs, and P25 without UV irradiation.

dx.doi.org/10.1021/cm200826c |*Chem. Mater.* 2011, 23, 3341–3347

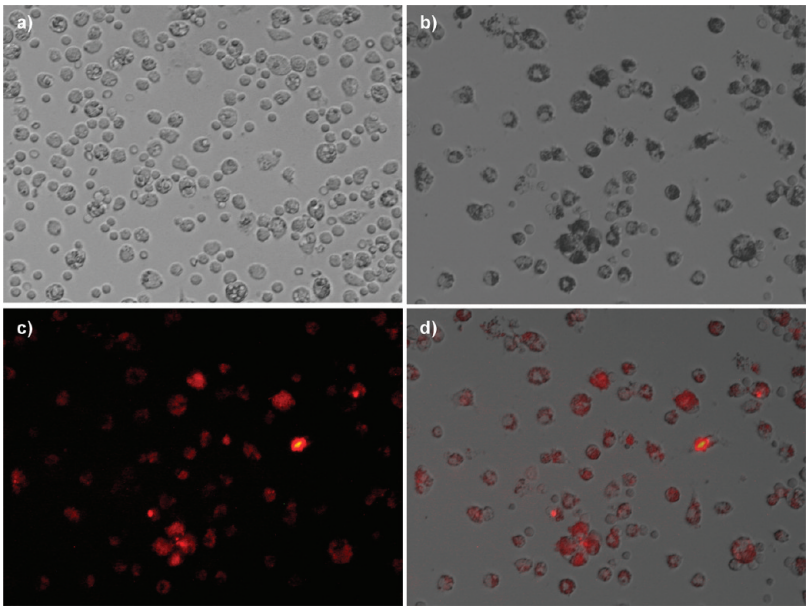

Figure 6. Cellular uptake of A/R NSs: (a) bright field image of intact macrophages; (b and c) bright field image and fluorescent image of macrophages treated with RB-modified A/R NSs, respectively; and (d) merged bright field and fluorescence image.

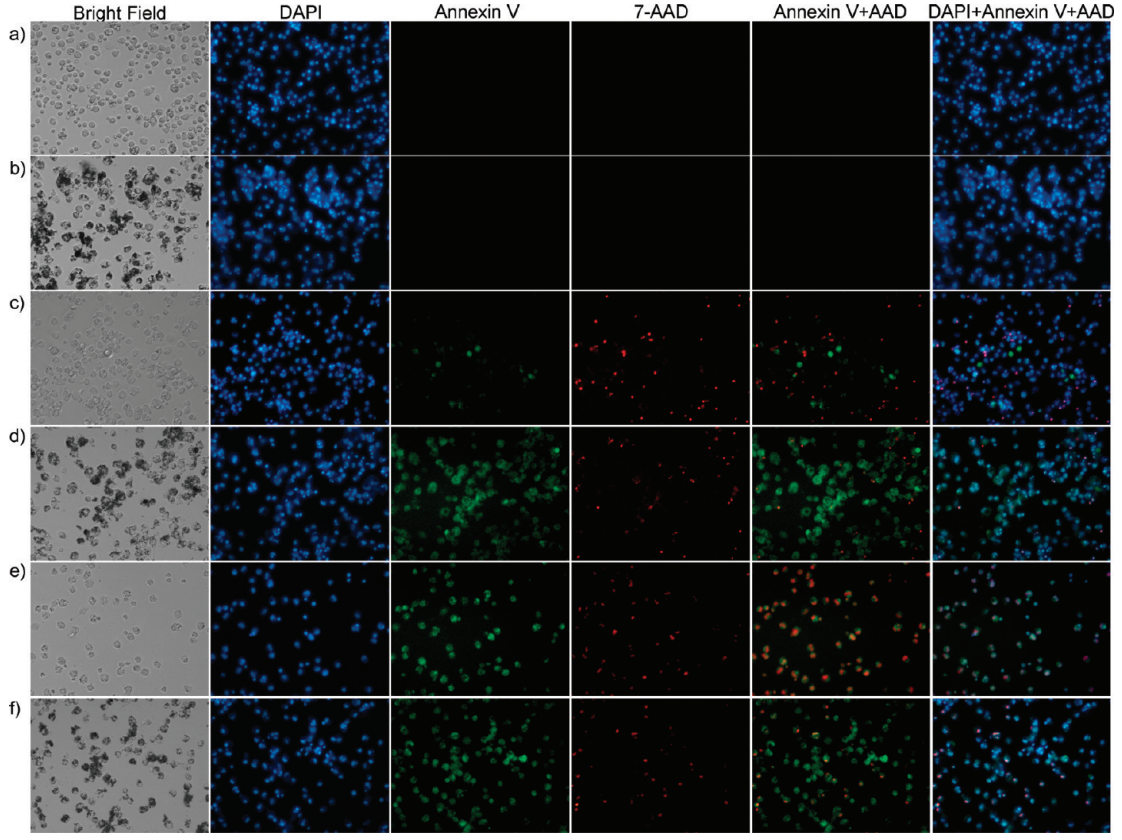

Figure 7. Fluorescence microscope images of cells treated with A/R NSs and exposed to UV light under the conditions summarized in Table 1. Panels a−f correspond to conditions a−f in Table 1. From left to right: bright field image; DAPI; annexin V; 7-AAD; merged image of annexin V and 7-AAD; and merged image of DAPI, annexin V, and 7-AAD.

30 min in the presence of A/R NSs caused 60% of the cells to die, even though the intensity of light was considerably less than that typically used for PDT (50−500 J/cm^2).[3] Thus, the A/R NSs are a promising photosensitizer for PDT.

Cellular Uptake of A/R NSs. A/R NSs were modified with a fluorescent dye (RB) to investigate their cellular uptake. Murine macrophages were then incubated with the RB-modified A/R NSs. The RB-modified A/R NSs were not observed outside the

dx.doi.org/10.1021/cm200826c |*Chem. Mater.* 2011, 23, 3341–3347

macrophages; therefore, they were entirely consumed by the macrophages (Figure 6). This demonstrates that the A/R NSs produced ROS that destroyed cells within the macrophages rather than outside them.

Identification of Apoptosis and Necrosis. The cause of death of the macrophages was investigated using fluorescent microscopic observations with an apoptosis detection reagent (annexin V-FITC, E_x/E_m = 495/519 nm) and necrosis detection reagent (7-aminoactinomycin D-Red, and 7-AAD-Red; E_x/E_m = 546/647 nm), as shown in Figure 7. Macrophages were incubated with A/R NSs for 24 h and then exposed to UV irradiation under one of the conditions described in Table 1 and the Experimental Methods section. Apoptosis is the naturally intended death of a cell, and necrosis is when the death of one cell unintentionally causes the death of those surrounding it. When a cell undergoes apoptotic death, phosphatidylserine (PS), which is usually stored on the inner (cytosolic) side of cell membranes, is no longer restricted to the cytosolic side of the membrane and becomes exposed at the surface of the cell. Annexin V has an affinity for PS and can therefore bind to apoptotic cells. However, PS is exposed at the surface of a cell in the cases of both apoptosis and necrosis; therefore, annexin V is not an absolute marker for apoptosis. 7-AAD has a strong affinity for DNA and does not readily pass through intact cell membranes. Cells with compromised membranes are stained with 7-AAD, whereas live cells with intact membranes remain unstained. Thus, 7-AAD can only stain necrotic cells. For these reasons, apoptotic cells are stained with annexin V and not 7-AAD, while necrotic cells are stained with either 7-AAD or both annexin V and 7-AAD. It should also be noted that 4′,6-diamidino-2-phenylindole (DAPI, E_x/E_m = 358/461 nm) can dye the DNA within the nucleus of a cell, regardless of its state. Thus, cells that are stained with DAPI but not with 7-AAD or annexin V are considered to be living cells. Figure 7a shows fluorescent images of untreated cells. These cells were stained with DAPI, but not with annexin V or 7-AAD, and were therefore live cells. For the same reasons, cells that were treated with A/R NSs were also live cells (Figure 7b). When untreated cells were exposed to UV light for 30 min, a small number of cells became stained with annexin V and 7-AAD (Figure 7c). As shown in the merged image of DAPI, annexin V, and 7-AAD, most cells remained unstained with annexin V and 7-AAD, and were only stained with DAPI. Thus, the majority of cells were living. Furthermore, because there were more cells stained with 7-AAD than annexin V, cell death was primarily caused by necrosis rather than apoptosis. In contrast, when the cells were treated with A/R NSs and exposed to UV light for 30 min, most cells died by apoptosis (Figure 7d). This is because a high yield of ROS was produced inside the cells; therefore, cell death was induced from within the cell. However, when A/R NSs were not present, applying UV irradiation yielded only a small amount of ROS that were outside the cells. These broke through the cell membrane and induced necrosis. UV irradiation for 90 min led to the destruction of most cells even without A/R NSs (Figure 7e). However, as observed in Figure 7c, the cells that were not treated with A/R NSs mainly died from necrosis. Cells were completely destroyed by treatment with A/R NSs and exposure to UV irradiation for 90 min (Figure 7f), and their death was induced primarily by apoptosis rather than necrosis, as shown in Figure 7d. The above results show that A/R NSs efficiently induce apoptosis only with UV irradiation, although Wang et al. demonstrated that ultrafine TiO_2 NPs induced apoptosis even without UV irradiation.[19] Ultrafine anatase TiO_2 NPs also induced splenocyte and hepatocyte apoptosis *in vivo* through mitochondria-mediated pathways without UV irradiation.[20−22] These findings imply that the use of A/R NSs in PDT affords a major advantage because cell death is induced only at areas exposed to UV light so that local treatment can be accomplished.

CONCLUSIONS

SA NPs, CFR NPs, and a mixture of SA and CFR NPs were synthesized in aqueous solution. Sea urchin-like A/R NSs combining SA and CFR NPs were produced through the self-assembly of JBU. The specific surface area of the A/R NSs was 220 m^2/g, which was considerably larger than those of SA NPs, CFR NPs, and P25. The amount of ROS yielded from the A/R NSs was significantly higher than that yielded from SA NPs, CFR NPs, and P25 because of their large surface area and the synergistic effect of the integration of anatase and rutile phases. The A/R NSs exhibited little cytotoxicity at concentrations less than 100 μg/mL, while the SA NPs, CFR NPs, and P25 showed some degree of cytotoxicity. Macrophages were killed more effectively by treatment with A/R NSs and UV irradiation than with P25 and UV irradiation. Furthermore, cells treated with A/R NSs and exposed to UV irradiation died mainly by apoptosis rather than necrosis, while cells that were not treated with A/R NSs died mainly from necrosis.

ASSOCIATED CONTENT

Supporting Information. Synthetic conditions used to prepare SA NPs, CFR NPs, and a mixture of SA and CFR NPs, XRD patterns of SA NPs, CFR NPs, and a mixture of SA and CFR NPs, and TEM images and SAED patterns of SA NPs, CFR NPs, and a mixture of SA and CFR NPs (PDF). This material is available free of charge via the Internet at http://pubs.acs.org.

AUTHOR INFORMATION

Corresponding Author
*E-mail: khayashi@basic.med.tokushima-u.ac.jp.

ACKNOWLEDGMENT

This work was supported by the Sasakawa Scientific Research Grant from The Japan Science Society.

REFERENCES

(1) Libby, P. *Nature* **2002**, *420*, 868.
(2) Hansson, G. K. *N. Engl. J. Med.* **2005**, *352*, 1685.
(3) Dougherty, T. J.; Gomer, C. J.; Henderson, B. W.; Jori, G.; Kessel, D.; Korbelik, M.; Moan, J.; Peng, Q. *J. Natl. Cancer Inst.* **1998**, *90*, 889.
(4) Roy, I.; Ohulchanskyy, T. Y.; Pudavar, H. E.; Bergey, E. J.; Oseroff, A. R.; Morgan, J.; Dougherty, T. J.; Prasad, P. N. *J. Am. Chem. Soc.* **2003**, *125*, 7860.
(5) Moan, J.; Iani, V.; Ma, L. W. . In *Photochemotherapy Photodynamic Therapy and Other Modalities. Proceedings of SPIE*; Ehrenberg, B., Jori, G., Moan, J., Eds.; **1996**; Vol. *2625*, p. 544.
(6) Rozhkova, E. A.; Ulasov, I.; Lai, B.; Dimitrijevic, N. M.; Lesniak, M. S.; Rajh, T. *Nano Lett.* **2009**, *9*, 3337.
(7) Songa, M.; Zhanga, R.; Daib, Y.; Gaob, F.; Chia, H.; Lva, G.; Chenb, B.; Wang, X. *Biomaterials* **2006**, *27*, 4230.
(8) Seo, J.-W.; Chung, H.; Kim, M.-Y.; Lee, J.; Choi, I.-H.; Cheon, J. *Small* **2007**, *3*, 850.

(9) Zheng, Z.; Huang, B.; Qin, X.; Zhang, X.; Dai, Y. *Chem.—Eur. J.* **2010**, *16*, 11266.
(10) Zachariah, A.; Baiju, K. V.; Shukla, S.; Deepa, K. S.; James, J.; Warrier, K. G. K. *J. Phys. Chem. C* **2008**, *112*, 11345.
(11) Li, G.; Ciston, S.; Saponjic, Z. V.; Chen, L.; Dimitrijevic, N. M.; Rajh, T.; Gray, K. A. *J. Catal.* **2008**, *253*, 105.
(12) Fang, Y.; Wu, Q.; Dickerson, M. B.; Cai, Y.; Shian, S.; Berrigan, J. D.; Poulsen, N.; Kröger, N.; Sandhage, K. H. *Chem. Mater.* **2009**, *21*, 5704.
(13) Katz, E.; Willner, I. *Angew. Chem., Int. Ed.* **2004**, *43*, 6042.
(14) Dickerson, M. B.; Sandhage, K. H.; Naik, R. R. *Chem. Rev.* **2008**, *108*, 4935.
(15) Chen, C.-L.; Rosi, N. L. *Angew. Chem., Int. Ed.* **2010**, *49*, 1924.
(16) Illeová, V.; Polakovič, M.; Štefuca, V.; Ačai, P.; Juma, M. *J. Biotechnol.* **2003**, *105*, 235.
(17) Chen, L.; Shen, Y.; Xie, A.; Huang, F.; Zhang, W.; Liu, S. *Cryst. Growth Des.* **2010**, *10*, 2073.
(18) Quevedo, J. A.; Omosebi, A.; Pfeffer, R. *AIChE J.* **2010**, *56*, 1456.
(19) Wang, J. J.; Sanderson, B. J. S.; Wang, H. *Mutat. Res. Genet. Toxicol. Environ. Mutagen.* **2007**, *628*, 99.
(20) Cui, Y.; Gong, X.; Duan, Y.; Li, N.; Hu, R.; Liu, H.; Hong, M.; Zhou, M.; Wang, L.; Wang, H.; Hong, F. *J. Hazard. Mater.* **2010**, *183*, 874.
(21) Li, N.; Ma, L.; Wang, J.; Zheng, L.; Liu, J.; Duan, Y.; Liu, H.; Zhao, X.; Wang, S.; Wang, H.; Hong, F.; Xie, Y. *Nanoscale Res. Lett.* **2010**, *5*, 108.
(22) Li, N.; Duan, Y.; Hong, M.; Zheng, L.; Fei, M.; Zhao, X.; Wang, J.; Cui, Y.; Liu, H.; Cai, J.; Gong, S.; Wang, H.; Hong, F. *Toxicol. Lett.* **2010**, *195*, 161.